HHS Public Access

Author manuscript

Cell Metab. Author manuscript; available in PMC 2017 December 13.

Published in final edited form as:

Cell Metab. 2016 December 13; 24(6): 848–862. doi:10.1016/j.cmet.2016.09.016.

Hepatocyte TAZ/WWTR1 Promotes Inflammation and Fibrosis in Nonalcoholic Steatohepatitis

Xiaobo Wang[1], **Ze Zheng**[1], **Jorge Matias Caviglia**[1,2], **Kathleen E. Corey**[3,4], **Tina M. Herfel**[5], **Ricard Masia**[4,6], **Raymond Chung**[3,4], **Jay H. Lefkowitch**[7], **Robert F. Schwabe**[1,2], and **Ira Tabas**[1,7,8,*]

[1]Department of Medicine, Columbia University, New York, NY 10032, USA

[2]Institute of Human Nutrition, Columbia University, New York, NY 10032, USA

[3]Gastrointestinal Unit, Massachusetts General Hospital, Boston, MA, 02114, USA

[4]Harvard Medical School, Boston, MA, USA

[5]Teklad Diets, Envigo, Madison, WI, 53713, USA

[6]Department of Pathology and Laboratory Medicine, Massachusetts General Hospital, Boston, MA, 02114, USA

[7]Department of Pathology and Cell Biology, Columbia University, New York, NY 10032, USA

[8]Department of Physiology and Cellular Biophysics, Columbia University, New York, NY 10032, USA

SUMMARY

Nonalcoholic steatohepatitis (NASH) is a leading cause of liver disease worldwide. However, the molecular basis of how benign steatosis progresses to NASH is incompletely understood, which has limited the identification of therapeutic targets. Here we show that the transcription regulator TAZ (WWTR1) is markedly higher in hepatocytes in human and murine NASH liver than in normal or steatotic liver. Most importantly, silencing of hepatocyte TAZ in murine models of NASH prevented or reversed hepatic inflammation, hepatocyte death, and fibrosis but not steatosis. Moreover, hepatocyte-targeted expression of TAZ in a model of steatosis promoted NASH features, including fibrosis. *In-vitro* and *in-vivo* mechanistic studies revealed that a key mechanism linking hepatocyte TAZ to NASH fibrosis is TAZ/TEA domain (TEAD)-mediated

*Correspondence: iat1@columbia.edu.

SUPPLEMENTAL INFORMATION

Supplemental Information includes nine figures, four tables, and Supplemental Experimental Procedures.

AUTHOR CONTRIBUTIONS

X.W., R.F.S., and I.T. developed the study concept and experimental design; X.W. performed all animal study procedures and most of the *in vitro* experiments; Z.Z. conducted the CHIP assays; J.M.C. conducted the fluorescence reporter mouse assay, hydroxyproline measurements, and αSMA IHC experiments. K.E.C., R.C., and J.H.L. collected and helped analyze the human samples; T.M.H. helped design the FPC diet; R.M. scored mouse liver for NASH features; and X.W., R.F.S., and I.T. interpreted the data and wrote the manuscript.

induction of Indian hedgehog (Ihh), a secretory factor that activates fibrogenic genes in hepatic stellate cells. In summary, TAZ represents a previously unrecognized factor that contributes to the critical process of steatosis-to-NASH progression.

eTOC blurb

Hepatic fibrosis is a key feature of nonalcoholic steatohepatitis (NASH), affecting morbidity. XXX et al investigate the underlying mechanisms for progression from benign steatosis to NASH and show that the transcription factor TAZ/WWTR1 is increased in mouse and human NASH. Silencing TAZ can prevent or reverse NASH features, notably fibrosis.

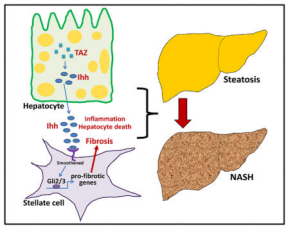

INTRODUCTION

The epidemic of obesity has led to the occurrence of fatty liver, or steatosis, in hundreds of millions of people worldwide. While simple steatosis is a relatively benign condition, approximately 20-30% of these subjects will develop liver inflammation, dysfunctional fibrosis, and hepatocyte death, a serious condition known as nonalcoholic steatohepatitis (NASH) (Rinella, 2015). NASH can progress to cirrhotic liver disease and hepatocellular carcinoma and has become the leading cause of liver failure (Corey and Kaplan, 2014; Rinella, 2015). Despite the high prevalence and clinical importance of NASH, many gaps remain in our understanding of its pathophysiology, leading to a lack of mechanism-based therapeutic targets and treatment options (White et al., 2012).

NASH most likely develops as a result of multiple hits (Day and James, 1998), including obesity/insulin resistance-mediated steatosis and other insults that promote inflammation, fibrosis, and hepatocyte death (Singh et al., 2015). However, the molecular mechanisms corresponding to these pathogenic processes and their integration are poorly understood. In particular, there is a great need to elucidate the mechanisms leading to hepatic fibrosis, which is the leading determinant of long-term mortality in patients with NASH (Angulo et al., 2015a; Angulo et al., 2015b; Puche et al., 2013). Extensive data indicate that activation of hepatic stellate cells (HSCs) plays a key role in NASH fibrosis (Mederacke et al., 2013), and although a number of factors have been proposed to activate HSCs in NASH, the work in this area is far from complete and has not yet led to FDA-approved treatment strategies (Angulo et al., 2015b; Puche et al., 2013).

In this context, we became interested in the Hippo pathway transcriptional activator TAZ (also known as WWTR1), which has been shown to have a pathophysiologic role in fibrosis in the lung (Liu et al., 2015). TAZ and the related protein YAP are orthologs of Drosophila *Yorkie*, a regulator of gene transcription that promotes tumor development in flies

(Zanconato et al., 2016; Zhao et al., 2010). Although the roles of TAZ/YAP in normal physiology in mammals appear modest, they have emerged as key factors in carcinogenesis, tumor progression, and metastasis. At a cell biological level, TAZ/YAP mediate cellular responses to both intracellular shape changes and changes in the extracellular matrix environment. In the basal state, TAZ/YAP are relatively inactive as nuclear transcriptional regulators, because kinases in the so-called Hippo pathway maintain TAZ/YAP in their phosphorylated, cytoplasmic state. Through dephosphorylation and other processes, however, TAZ/YAP translocate to the nucleus and become active transcriptional regulators. In the nucleus, they interact with TEA domain (TEAD) proteins, leading to transcription of genes possessing consensus TEAD-binding *cis*-regulatory sequences in promoter and enhancer regions.

While there are some hints in the literature that TAZ or YAP may be involved in various liver processes, their possible role in fatty liver disease or NASH progression has not been reported. We now demonstrate that TAZ expression is elevated in the livers of humans with NASH-related fibrosis and in the livers of several murine NASH models. Silencing of hepatocyte Taz in NASH mice prevents and even reverses the development of liver inflammation and fibrosis without affecting steatosis, and forced expression of TAZ in hepatocytes can promote the progression of NASH from steatosis. *In vitro*, conditioned medium from Taz-silenced *vs*. control hepatocytes decreases fibrotic responses in hepatic stellate cells (HSCs), which we link both *in vitro* and *in vivo* in murine NASH to decreased hepatocyte secretion of the TAZ/TEAD target Indian hedgehog (Ihh). Thus, TAZ promotes NASH progression, including fibrosis, and therefore emerges as a potential therapeutic target to prevent the progression of steatosis to NASH.

RESULTS

TAZ Levels are Increased in the Livers of Humans and Mice with NASH

We conducted TAZ immunofluorescence microscopy on human liver samples from obese individuals with normal, steatotic, and NASH histology. While there was similar TAZ staining in normal and steatotic livers, we observed a significant increase in TAZ staining in the NASH samples (Figure 1A). The specificity of the anti-human TAZ antibody for immunofluorescence is demonstrated by an siTaz experiment conducted with human HepG2 liver cells (Figure S1A). TAZ localization in NASH liver was not confined to any one zone (Figure S1B), and most of the TAZ-stained cells were hepatocytes, as identified by HNF4α staining (Figure S1C). We then analyzed TAZ protein by immunoblot in liver extracts from subjects with NASH *vs*. early NAFLD and normal liver and found that TAZ was expressed at the highest level in NASH liver (Figure 1B).

In preparation for TAZ causation studies, we explored TAZ expression in various mouse models of NASH. We began with the widely used methionine/choline-deficient (MCD) diet model, which induces NASH-like liver pathology despite weight loss and insulin sensitivity (Hebbard and George, 2011), and found that TAZ expression was markedly higher in MCD liver compared with control liver (Figure 1C). We next sought to study TAZ in a NASH model that had weight gain and insulin resistance, as is the case with humans. For this purpose, we modified two previously described diet-induced weight-gain models (Charlton

et al., 2011; Kohli et al., 2010) to achieve NASH features within an experimentally acceptable time frame. We devised a diet that was rich in fructose, palmitate, cholesterol (FPC), and trans-fat, with other features as detailed in Tables S1 and S2. Cholesterol (1.2% by wt) was added to the diet in view of multiple links between liver cholesterol and NASH in humans (Ioannou, 2016). Note that a high dietary content of cholesterol is needed to achieve adequately increased cholesterol absorption in C57BL/6J mice, the strain used here (Jolley et al., 1999).

After 16 weeks, FPC-fed mice had higher body weight and liver:body weight ratio than chow-fed mice (Figure S2A-B). Additionally, FPC mice showed significant increases in fasting blood glucose, plasma insulin, and alanine aminotransferase (ALT) and aspartate aminotransferase (AST) levels (Figures S2C-E). Analyses of liver sections revealed that the following parameters were greater in the livers of FPC-fed mice *vs*. chow-fed mice: lipid droplet area (H&E and Oil Red O [ORO]), inflammatory cells, fibrosis (aniline blue component of trichrome [Trichr] and Sirius red [Sir red]), and cell death (TUNEL) (Figures S2F-K). As further evidence of inflammation, FPC liver had elevated liver mRNA levels for *Tnfa*, *Mcp1*, *F4/80* (*Adgre1*; macrophages) and a higher percentage of F4/80$^+$ cells (Figures S2L-M). With regard to fibrosis-associated parameters, hepatic *Tgfb1* and *Acta2* (α-smooth muscle actin, α-SMA) mRNAs were higher in FPC-fed mice compared with chow-fed mice (Figure S2N), and there was also an increase in α-SMA$^+$ cells (Figures S2O). Moreover, as designed, liver cholesterol was elevated in the livers of FPC mice (Figure S2P-Q). Additional features of the model in terms of blood parameters and liver assays are shown in Figure S3, and Table S3 shows hepatic fatty acid changes similar to those reported for human NASH liver (Yamada et al., 2015). Finally, Figure S4A-G shows a direct comparison with one of the models from which it was derived, referred to as the “fast food” (FF) model (Charlton et al., 2011).

Most importantly for the purpose of our study, the livers of FPC mice express high levels of TAZ protein and *Wwtr1* (Taz) mRNA (Figures 1D-E). By immunoblot analysis, TAZ was abundant in extracts of primary hepatocytes from FPC-fed mice, but it could not be detected in extracts of combined non-hepatocytes (Figure S4H). Moreover, in view of the fact that the transcriptionally active form of TAZ is non-phosphorylated and nuclear (Liu et al., 2011), we found that the livers of FPC-fed mice had a lower phospho-TAZ:total TAZ ratio and higher nuclear TAZ compared with the livers of chow-fed mice (Figure S4I-J). Collectively, these data show that hepatocyte TAZ is induced in the livers of humans and mice with NASH, which led us to explore the possibility that TAZ may be a contributor to the progression from benign steatosis to NASH.

TAZ Silencing in Hepatocytes Suppresses Liver Inflammation, Fibrosis, and Cell Death in Mouse Models of NASH

To study TAZ function in NASH development, we ligated shTaz to a vector developed to silence genes in liver, AAV8-H1 (Lisowski et al., 2014). (NB: To conform to the literature, we use the common name Taz, rather than *Wwtr1*, for sh terminology.) AAV8-H1-shTaz led to robust silencing of TAZ (Figure 2A) and a decrease in the known TAZ/TEAD transcriptional targets, *Birc5* and *Rhamm* (Figure S5A). In terms of specificity within the

liver, note that TAZ expression in NASH liver was abundant in hepatocytes but not detected by immunoblot in combined non-hepatocytes (above). In extracts of adipose, heart, lung, and skeletal muscle, TAZ was not decreased in mice treated with AAV8-H1-shTaz; note that TAZ was not detected in kidney extract (Figure S5B).

Mouse body weight, liver:body weight ratio, fasting blood glucose, plasma insulin, and plasma cholesterol were similar in the shTaz and control groups (Figure S5C-G). Liver sections showed marked reductions in both inflammatory cell infiltration and fibrosis endpoints in the shTaz cohort (Figure 2B-D), as reflected in fibrosis stage and NAFLD activity score (NAS) (Figure S5H-I), while steatosis was not affected (Figure S5J). Plasma ALT was decreased in shTaz-treated mice (Figure 2E), and this was associated with a decrease in TUNEL+ and 4-HNE+ liver cells (Figure 2F and S5K), indicating that Taz silencing reduced both cell death and oxidative stress in liver cells. At the mRNA level, Taz silencing caused a robust reduction in the expression of mRNAs related to hepatic inflammation—*Tnfa*, *Mcp1*, and *F4/80* (*Adgre1*)—and fibrosis (Figure 2G-H), including the NASH-relevant genes *Acta2* (α-SMA), *Timp1*, *Des*, *Col1a1*, *Col1a2*, *Col3a1*, and *Vim* (Friedman, 2008; Younossi et al., 2011). These changes were accompanied by decreases in both F4/80$^+$ macrophages and α-SMA$^+$ cells (Figures 2I-J and S5L). Note that silencing TAZ did not change filipin staining of liver, suggesting that TAZ is downstream of liver cholesterol accumulation (Figure S5M).

We conducted a similar study in which hyperphagic *Mc4r*$^{-/-}$ mice (Butler and Cone, 2002) were fed the FPC diet for 16 wks. These mice develop more liver fibrosis compared with FPC-fed WT C57BL/6J mice, and silencing of Taz in the liver of these mice resulted in decreased staining for aniline blue, Sirius red, and α-SMA; lower hydroxyproline content; and decreased liver inflammation (Figure S6). We confirmed these results in the MCD model, where AAV8-H1-shTaz decreased both hepatic inflammation and fibrosis without affecting steatosis and also reduced inflammatory and fibrotic gene expression, α-SMA$^+$ cells, and macrophages in the liver (Figure S7A-J). In contrast, in a model of liver fibrosis in which TAZ is not increased in the liver—CCl4-treated mice—silencing Taz did not suppress fibrosis or fibrotic gene expression (Figure S7K-M). We also conducted an experiment in MCD-fed *Wwtr1*$^{fl/fl}$ mice (Xin et al., 2013) treated with AAV8-TBG-LacZ control or AAV8-TBG-Cre, which deletes floxed genes specifically in hepatocytes *vs.* other types of liver cells (Mu et al., 2015) or other organs (Figure S8A-B). As above, inflammatory endpoints, α-SMA$^+$ cells, fibrosis-related gene expression, and cell death were decreased by hepatocyte TAZ knockdown, as was fibrosis itself, despite the fact that the level of fibrosis in the control cohort in this particular experiment was less than usual (Figure S8C-H).

We next asked whether features of NASH, notably fibrosis, could be reversed by treating mice with AAV8-H1-shTaz after NASH had developed. For this purpose, mice were placed on the FPC diet for 16 wks, treated with shTaz or control vector, then continued on the diet for an additional 12 weeks. As expected for 28 weeks of FPC feeding, the control mice had marked inflammation and fibrosis, and all parameters were decreased by Taz silencing (Figure 3). Thus, in separate models of NASH, hepatic TAZ silencing improved or reversed key liver parameters related to inflammation, fibrosis, and cell death without affecting metabolic parameters.

TAZ Silencing in Hepatocytes Blocks Steatosis-to-NASH Progression, and Genetically Induced TAZ Expression in Hepatocytes Promotes NASH in a Mouse Model of Steatosis

To investigate the role of TAZ specifically in steatosis-to-NASH progression, mice were first fed the FPC diet for 8 weeks and then injected with AAV8-H1-shTaz or control virus, followed by an additional 8 weeks on the diet. After 8 weeks, there was only a very slight increase in hepatic TAZ compared with mice fed the FPC diet for 16 weeks, and the livers showed steatosis but no appreciable inflammation or fibrosis (Figure 4A-B). The livers of mice who received shTaz at week 8 showed marked reductions at 16 weeks in fibrosis endpoints, inflammatory cells, inflammatory- and fibrosis-related genes, $F4/80^+$ macrophages, and α-SMA^+ cells, but not steatosis, and plasma ALT was also decreased by shTaz (Figure 4B-H). These data suggest that TAZ is particularly important in the critical processes that promote steatosis-to-NASH progression.

Finally, whereas the above experiments addressed necessity of TAZ in NASH, we addressed the question of sufficiency by treating mice on the aforementioned FF diet, which is a model of steatosis in the time frame studied (above), with AAV8-albumin-TAZ. We achieved a level of hepatic TAZ protein in these mice that was similar to that in FPC-fed mice, and this was associated with an increase in all parameters of inflammation and fibrosis (Figure S9). Thus, TAZ is both necessary and sufficient to promote the development of NASH in mice.

Hepatocyte TAZ Induces Indian Hedgehog, Which Promotes the Expression of Pro-Fibrotic Genes in Hepatic Stellate Cells and Mediates TAZ-Induced NASH

We sought to explore possible mechanisms linking TAZ to fibrosis progression. Previous studies have demonstrated that HSCs, the main source of collagen-producing myofibroblasts in NASH-related fibrosis (Mederacke et al., 2013), can be activated by the hedgehog pathway (Angulo et al., 2015b). In this context, ChIP array data suggested that the gene encoding Indian hedgehog, *Ihh*, is a TAZ/TEAD target. We therefore considered the hypothesis that increased TAZ in hepatocytes during NAFLD progression leads to the secretion of Ihh, which then acts on HSCs to promote the expression of pro-fibrotic genes.

To begin, we conducted TAZ ChIP analysis of livers of chow-fed and FPC-fed mice with or without TAZ silencing, focusing on a TAZ/TEAD consensus sequence in intron 1 of murine *Ihh* that is conserved among species, including humans (Zanconato et al., 2015) (Figure 5A-B). The results show a significant increase in the ChIP signal in the livers of FPC-fed *vs.* chow-fed mice, which was dependent on anti-TAZ and was not seen when a non-consensus sequence was amplified. Most importantly, the ChIP signal in the livers of FPC mice was lowered to the chow level by TAZ silencing. Next, we conducted a dual-luciferase reporter assay using this intron 1 consensus sequence *vs.* a mutated sequence, with 500 bp of upstream and downstream flanking sequence. The luciferase vectors were transfected into shControl- or shTaz-treated AML12 cells, a non-cancerous mouse hepatocyte cell line (Dumenco et al., 1995). The data showed robust luciferase activity with the consensus sequence *vs.* mutated sequence in control AML12 cells, with a marked decrease in siTaz-treated cells (Figure 5C). Thus, TAZ interacts with a TAZ/TEAD consensus sequence in intron 1 of *Ihh* in the livers of FPC-fed mice, and this sequence can drive gene expression in a TAZ-dependent manner.

We next asked whether human NASH liver expressed higher levels of Ihh than normal and steatotic liver. As was the case with TAZ (above), the expression of Ihh was greater in NASH liver than in normal and steatotic liver (Figure 5D). Similarly, the livers of FPC-fed mice had markedly higher levels of Ihh compared with the livers of chow-fed mice (Figure 5E). We then compared chow and FPC liver extracts for gene expression of *Ihh* and the Ihh pathway downstream genes, Gli2 and Gli3. All three mRNAs were elevated in FPC liver, as was an Ihh target gene, osteopontin (*Opn*) (Razzaque et al., 2005), which is involved in HSC-induced fibrosis in NASH (Syn et al., 2011) (Figure 5F). To explore causation with regard to TAZ, we repeated these assays in FPC-fed mice with or without TAZ silencing. All four mRNAs and Ihh protein were substantially lower in the TAZ-silenced mice (Figure 5G-H), as was OPN as assessed by immunohistochemistry (Figure 5I). Thus, TAZ induces transcriptionally active Ihh during NASH progression in FPC-fed mice, and one of the targets of Ihh, *Opn*, has been linked to NASH fibrosis (Bohinc and Diehl, 2012; Syn et al., 2011).

To explore the possibility that TAZ-induced Ihh is secreted by hepatocytes and activates HSCs, we moved to an *in vitro* model using both AML12 cells and primary murine HSCs. Consistent with our data *in vivo*, siTaz treatment of AML12 cells lowered cellular *Ihh* mRNA in the cells and Ihh protein in both the cells and media (Figure 6A-C). We then added conditioned medium (CM) from control or Taz-silenced AML12 cells, as well as medium not exposed to cells (non-CM), to primary murine hepatic stellate cells (HSCs). Compared with non-CM, hepatocyte CM markedly increased *Opn* mRNA as well as the mRNAs for two proteins involved in fibrosis, *Timp1* and *Col1a1*. Most importantly, CM from TAZ-silenced hepatocytes lowered the levels these mRNAs and protein compared to CM from control hepatocytes (Figure 6D). Conditioned medium from *Ihh*-silenced hepatocytes also decreased the three mRNAs in HSCs (Figure 6E), although the absolute degree of *Timp1* lowering was somewhat greater in this experiment than in the siTaz experiment. Finally, to make a more direct link between TAZ-induced Ihh in hepatocytes and activation of HSCs, we restored Ihh in siTaz-treated hepatocytes by Ihh transfection and then asked whether this lessened the suppressive effect of CM from these cells on the expression of the fibrosis-related genes in HSCs. Transfection of TAZ-silenced hepatocytes with Ihh led to a level of Ihh in the CM that was similar to that in the CM of control hepatocytes (Figure 6F—compare 1st and 4th bars). As before, the CM of TAZ-silenced hepatocytes suppressed *Opn*, *Timp1* and *Col1a1* mRNA in HSCs (Figure 6G—compare 2nd and 4th bars), and we found that restoration of *Ihh* in these TAZ-silenced cells rescued CM-induced HSC gene expression (Figure 6G—compare 4th and 5th bars). Finally, we wondered whether TAZ might also directly regulate fibrogenic gene expression or proliferation in HSCs. However, we found that silencing of Taz in primary HSCs affected neither fibrogenic gene expression nor cell proliferation (Figure 6H). Together, these studies suggest that hepatocyte induced Ihh in hepatocytes promotes the expression of pro-fibrotic genes in HSCs.

To provide causation evidence *in vivo* for the role Ihh in TAZ-induced NASH, we first used AAV8-*Ihh* to restore Ihh in *Taz*-silenced FPC-fed mice. As designed, the level of hepatic *Ihh* mRNA in Ihh-restored shTaz mice was similar to that in control mice (Figure 7A, first set of bars). Consistent with the TAZ-Ihh hypothesis, Ihh restoration prevented the improvement in

all NASH features that we see with Taz silencing, including liver inflammation, fibrosis and fibrogenic mRNA expression, and cell death (Figure 7A-D). Next, we directly silenced Ihh in FPC-fed mice using AAV8-H1-sh*Ihh* and found that this intervention, like silencing Taz, improved all NASH-like features (Figure 7E-L). These combined *in vitro* and *in vivo* data support the conclusion that hepatocyte TAZ promotes NASH progression in large part through inducing Ihh.

DISCUSSION

NASH, characterized by inflammation, cell death, and fibrosis can progress to advanced liver disease, cirrhosis, and the need for liver transplant. Steatosis alone is believed to be a little to no risk for progressive liver disease. Given the clinical significance of NASH compared to steatosis (Rinella, 2015), a critical objective of research in this area is to identify factors and pathways that promote the conversion of steatosis to NASH and the development of fibrosis. The importance of this objective is underscored by the fact that NASH is becoming the leading cause of liver disease worldwide and yet lacks any definitive, evidence-based drug therapies approved by the US Food and Drug Administration (Rinella, 2015). In this context, the finding that a hepatocyte TAZ-Ihh pathway plays a key role in steatosis-to-NASH conversion and the development of fibrosis provides new insight into NASH and may suggest new targets for therapy.

Hepatic fibrosis is a key feature of NASH that distinguishes it from steatosis and determines long-term mortality in patients with NASH (Angulo et al., 2015a). While both TAZ and YAP have been implicated in organ fibrosis in other settings, particularly in the lung with links to TGFβ-SMAD signaling or induction of plasminogen activator inhibitor-1 (Liu et al., 2015; Mitani et al., 2009; Piersma et al., 2015; Saito and Nagase, 2015), there are only scattered reports about their roles in liver fibrosis, and none in the setting of NAFLD. For example, a recent study reported an association between microRNA-130/301, which can regulate TAZ and YAP, and CCl_4-induced liver fibrosis (Bertero et al., 2015), but there were no direct causation or mechanistic data related to the role of TAZ in this process, and we now show that TAZ is not involved in CCl_4-induced liver fibrosis. Another report showed that knockout of a pair of Hippo factors called Mps One Binder Kinase Activator (MOB)1A/1B in lean, non-NASH mice caused elevated TGFβ-2/3 and liver fibrosis in a manner that was partially dependent on TAZ (Nishio et al., 2016).

Although the mechanism of TAZ in liver fibrosis in NASH is likely to be multifactorial, we show here that the TAZ target Ihh is elevated in human and mouse NASH liver in a TAZ-dependent manner and is important in NASH progression and fibrosis. Previous work has implicated hedgehog signaling in NASH fibrosis, particularly *Shh* signaling in HSCs (Bohinc and Diehl, 2012), both directly and via the induction of the pro-fibrotic cytokine IL-13 by immune cells (Shimamura et al., 2008; Syn et al., 2010). ChIP array data (Zhao et al., 2008) suggested to us that *Ihh* might be a TAZ/TEAD target gene by interacting with a consensus site in intron 1 of the *Ihh* gene, which we have now confirmed using complementary ChIP and luciferase reporter assays. Most importantly, hepatocyte TAZ-induced *Ihh* activated a fibrosis program in HSCs in cell culture, restoration of Ihh in

hepatocyte-TAZ-silenced mice restored NASH progression, and direct silencing Ihh in hepatocytes suppressed NASH.

Two other critical features of NASH, inflammation and cell death, were also ameliorated by TAZ silencing in our study. Little is known about the pro-inflammatory roles of TAZ, and, in general, YAP and TAZ inhibit rather than promote apoptosis during development and in cancer (Yu et al., 2015). However, there is one report showing that siTaz decreased TNFα-induced apoptosis in salivary gland epithelial cells (Hwang et al., 2014). RIP3-mediated necroptosis may also be important in hepatocyte death in NASH (Gautheron et al., 2014), and therefore it is possible that TAZ promotes this pathway. Given the various consequences of cell necrosis, this action of TAZ could contribute to inflammation and fibrosis as well as cell death in NASH (Chan et al., 2015; Luedde et al., 2014).

Our study focused on TAZ in hepatocytes, but a recent report showed that YAP was significantly increased in progenitor-like reactive-appearing ductular cells (RDCs) in human and mouse NASH liver (Machado et al., 2015). We also found increased YAP in the livers of FPC mice, and consistent with the data of Machado et al., most of the YAP-positive cells did not colocalize with HNF4α-positive hepatocytes (data not shown). While the role of YAP in NASH remains to be elucidated, the authors showed correlations among YAP^+ RDCs, fibrosis, accumulation of myofibroblasts, and expression of *Shh* and *Opn*. Of note, silencing TAZ in the livers of FPC mice did not affect YAP expression (data not shown).

Most of our experiments were conducted in a mouse model of insulin resistance and NAFLD that was a modification of previously described models (Charlton et al., 2011; Kohli et al., 2010). The diet was based on human dietary risk factors for NASH, and the key improvement over previous models was the development of inflammation, hepatocyte death, and fibrosis in 16 weeks without the need for genetically engineered mutations and in the background of weight gain and insulin resistance. Whereas the fructose component of the diet likely contributes to steatosis (Abdelmalek et al., 2010; Ishimoto et al., 2013), the cholesterol and palmitic acid components may be important in NASH progression and perhaps TAZ induction. The accumulation of unesterified cholesterol in the liver has been implicated in the development of NASH in humans (Ioannou, 2016) and in various mouse models (Subramanian et al., 2011; Van Rooyen et al., 2011; Wouters et al., 2008). For example, studies using mice fed high-cholesterol diets have suggested that cholesterol can directly activate HSCs by inducing TLR4, promote oxidative stress and cell death in hepatocytes via excess mitochondrial cholesterol, and promote inflammation in Kupffer cells through lysosomal cholesterol enrichment (Bieghs et al., 2013; Rawson, 2006; Teratani et al., 2012). If increased liver cholesterol is important in TAZ induction in NASH, further studies will be needed to define the mechanisms. Likewise, palmitic acid has been reported to induce pro-inflammatory cytokine production by hepatocytes and Kupffer cells during NASH (Joshi-Barve et al., 2007; Miura et al., 2013), but other mechanisms may be involved as well.

In summary, we show that the Hippo pathway transcription factor TAZ and its gene target Ihh are elevated in the livers of humans with NASH, which is recapitulated in mouse models. In these models, silencing of TAZ or Ihh suppresses key features of NASH

progression but not steatosis. Moreover, silencing TAZ after NASH has developed can partially reverse NASH features, including fibrosis. Although further mechanistic work is needed to fully understand these new findings, the data provide new insight into the pathophysiology of NASH and raise the possibility of liver-directed TAZ inhibition as a new therapeutic strategy to prevent NASH progression.

EXPERIMENTAL PROCEDURES

Animal Studies

Male wild-type mice C57BL/6J (#000664, 8-10 weeks/old) and MC4R-negative *loxTB Mc4r* mice (#006414, 6 weeks/old), referred to here as *Mc4r*$^{-/-}$ mice, were obtained from Jackson Laboratory (Bar Harbor, ME) and were allowed to adapt to housing in the Columbia University Medical Center Institute of Comparative Medicine for 1 week prior to random assignment to experimental cohorts. The mice were then fed the following diets for the times indicated in the figure legends: (a) chow diet (Picolab rodent diet 20, #5053); (b) “fast-food” (FF) diet (TestDiet 1810060): high-fat diet with drinking water containing 42 g/L glucose and fructose (55%/45%, w/w); or (c) fructose-palmitate-cholesterol (“FPC”) diet (Teklad, TD.140154): similar to FF diet but with 1.25% added cholesterol and with palmitic acid, anhydrous milk fat, and Primex as the sources of fat and with a ~60% decrease in vitamin E and a ~35% decrease in choline compared with typical mouse diets. The detailed composition of these diets appear in Tables S1 and S2. For several experiments, groups of mice were placed on a methionine-choline-deficient diet (Teklad, TD. 90262) for 8 weeks, as described (Dixon et al., 2012). Adeno-associated virus (2×10^{11} genome copy/mouse) was delivered by tail vein injection either 1 week prior to diet initiation or after 8 or 16 weeks of the FPC diet. For CCl_4-induced liver fibrosis, 6 week/old C57BL/6J mice were injected i.p. biweekly for 6 weeks with 0.5 μl/g body weight of CCl_4, which was dissolved in olive oil at a ratio of 1:3 (Mederacke et al., 2013). For the imaging of organs undergoing AAV8-TBG-Cre-mediated recombination, ZsGreen reporter mice (#007906, Jackson Laboratory) (Mu et al., 2015) were injected i.v. with AAV8-TBG-Cre (1×10^{11} genome copies/mouse). One week later, the mice were sacrificed, and selected organs were fixed and then imaged using a Leica MZ 16F fluorescence stereomicroscope. Animals were housed in standard cages at 22°C in a 12-12-h light -dark cycle. All animal experiments were performed in accordance with institutional guidelines and regulations and approved by the Institutional Animal Care and Use Committee at Columbia University.

Human Samples

Liver biopsy specimens from individuals undergoing weight loss surgery were selected from the MGH NAFLD Biorepository. Patients gave informed consent at the time of recruitment, and their records were anonymized and de-identified. Studies were approved by the Partners Human Research Committee (IRB) and conducted in accordance with National Institutes of Health and institutional guidelines for human subject research. Additional anonymized and de-identified liver biopsy sections were obtained from Dr. Jay Lefkowitch, Columbia University Medical Center. Cases with NAFLD activity score (NAS) of 1-3 were classified as early NAFLD (no fibrosis), while cases with NAS ≥5 and fibrosis stage 1a/b-4 were

classified as NASH. Cases with steatosis score ≥1 and inflammation and ballooning scores of 0 and no fibrosis were classified as steatosis. Cases with NAS 0 were classified as normal.

Blood and Plasma Analyses

Fasting blood glucose was measured using a glucose meter (One Touch Ultra, Lifescan) in mice that were fasted for 4-5 h, with free access to water. Complete blood counts were obtained with the FORCYTE Veterinary Hematology Analyzer (Oxford Science, Inc.). Total plasma triglyceride and cholesterol were assayed using a commercially available kit from Wako. For insulin, MCP1, AST, ALT, TC, TG are measured following kit instruction by using plasma.

Statistical Analysis

All results are presented as mean ± SEM. P values were calculated using the Student's t-test for normally distributed data and the Mann-Whitney rank sum test for non-normally distributed data. One-way ANOVA with post-hoc Tukey test was used to evaluate differences among groups when 3 or more groups were analyzed.

Supplementary Material

Refer to Web version on PubMed Central for supplementary material.

ACKNOWLEDGMENTS

We thank Dr. Utpal Pajvani, Columbia University, for helpful discussions; Dr. Yuri Choi, Massachusetts General Hospital, for assisting with the human liver samples; Dr. Stephen M. Lagana, Columbia University, for human NASH liver histology analysis; Dr. Hongfeng Jiang for the liver lipid profiling; and Dr. Peter Nagy, Columbia University, for assisting with the ChIP experiments. This work was supported by NIH grants HL087123 and HL075662 to I.T; DK078772 to R.T.C; DK99422 to K.E.C.; and R03DK101863 to J.M.C. Z.Z. is a Russell Berrie Foundation Scholar in Diabetes Research. The liver lipid profiling work was supported by NIH Grant Number UL1 TR000040 from the National Center for Advancing Translational Science.

REFERENCES

Abdelmalek MF, Suzuki A, Guy C, Unalp-Arida A, Colvin R, Johnson RJ, Diehl AM, Nonalcoholic Steatohepatitis Clinical Research, N. Increased fructose consumption is associated with fibrosis severity in patients with nonalcoholic fatty liver disease. Hepatology. 2010; 51:1961–1971. [PubMed: 20301112]

Angulo P, Kleiner DE, Dam-Larsen S, Adams LA, Bjornsson ES, Charatcharoenwitthaya P, Mills PR, Keach JC, Lafferty HD, Stahler A, et al. Liver Fibrosis, but No Other Histologic Features, Is Associated With Long-term Outcomes of Patients With Nonalcoholic Fatty Liver Disease. Gastroenterology. 2015a; 149:389–397. e310. [PubMed: 25935633]

Angulo P, Machado MV, Diehl AM. Fibrosis in nonalcoholic Fatty liver disease: mechanisms and clinical implications. Semin Liver Dis. 2015b; 35:132–145. [PubMed: 25974899]

Bataller R, Schwabe RF, Choi YH, Yang L, Paik YH, Lindquist J, Qian T, Schoonhoven R, Hagedorn CH, Lemasters JJ, et al. NADPH oxidase signal transduces angiotensin II in hepatic stellate cells and is critical in hepatic fibrosis. J Clin Invest. 2003; 112:1383–1394. [PubMed: 14597764]

Bertero T, Cottrill KA, Annis S, Bhat B, Gochuico BR, Osorio JC, Rosas I, Haley KJ, Corey KE, Chung RT, et al. A YAP/TAZ-miR-130/301 molecular circuit exerts systems-level control of fibrosis in a network of human diseases and physiologic conditions. Sci Rep. 2015; 5:18277. [PubMed: 26667495]

Bieghs V, Hendrikx T, van Gorp PJ, Verheyen F, Guichot YD, Walenbergh SM, Jeurissen ML, Gijbels M, Rensen SS, Bast A, et al. The cholesterol derivative 27-hydroxycholesterol reduces steatohepatitis in mice. Gastroenterology. 2013; 144:167–178. e161. [PubMed: 23041327]

Bohinc BN, Diehl AM. Mechanisms of disease progression in NASH: new paradigms. Clin Liver Dis. 2012; 16:549–565. [PubMed: 22824480]

Butler AA, Cone RD. The melanocortin receptors: lessons from knockout models. Neuropeptides. 2002; 36:77–84. [PubMed: 12359499]

Chan FK, Luz NF, Moriwaki K. Programmed necrosis in the cross talk of cell death and inflammation. Annu Rev Immunol. 2015; 33:79–106. [PubMed: 25493335]

Chang TC, Wentzel EA, Kent OA, Ramachandran K, Mullendore M, Lee KH, Feldmann G, Yamakuchi M, Ferlito M, Lowenstein CJ, et al. Transactivation of miR-34a by p53 broadly influences gene expression and promotes apoptosis. Mol Cell. 2007; 26:745–752. [PubMed: 17540599]

Charlton M, Krishnan A, Viker K, Sanderson S, Cazanave S, McConico A, Masuoko H, Gores G. Fast food diet mouse: novel small animal model of NASH with ballooning, progressive fibrosis, and high physiological fidelity to the human condition. Am J Physiol Gastrointest Liver Physiol. 2011; 301:G825–834. [PubMed: 21836057]

Corey KE, Kaplan LM. Obesity and liver disease: the epidemic of the twenty-first century. Clin Liver Dis. 2014; 18:1–18. [PubMed: 24274861]

Day CP, James OF. Steatohepatitis: a tale of two “hits”? Gastroenterology. 1998; 114:842–845. [PubMed: 9547102]

Dixon LJ, Berk M, Thapaliya S, Papouchado BG, Feldstein AE. Caspase-1-mediated regulation of fibrogenesis in diet-induced steatohepatitis. Lab Invest. 2012; 92:713–723. [PubMed: 22411067]

Dumenco L, Oguey D, Wu J, Messier N, Fausto N. Introduction of a murine p53 mutation corresponding to human codon 249 into a murine hepatocyte cell line results in growth advantage, but not in transformation. Hepatology. 1995; 22:1279–1288. [PubMed: 7557882]

Friedman SL. Mechanisms of hepatic fibrogenesis. Gastroenterology. 2008; 134:1655–1669. [PubMed: 18471545]

Gautheron J, Vucur M, Reisinger F, Cardenas DV, Roderburg C, Koppe C, Kreggenwinkel K, Schneider AT, Bartneck M, Neumann UP, et al. A positive feedback loop between RIP3 and JNK controls non-alcoholic steatohepatitis. EMBO Mol Med. 2014; 6:1062–1074. [PubMed: 24963148]

Hebbard L, George J. Animal models of nonalcoholic fatty liver disease. Nat Rev Gastroenterol Hepatol. 2011; 8:35–44. [PubMed: 21119613]

Hwang SM, Jin M, Shin YH, Ki Choi S, Namkoong E, Kim M, Park MY, Park K. Role of LPA and the Hippo pathway on apoptosis in salivary gland epithelial cells. Exp Mol Med. 2014; 46:e125. [PubMed: 25502757]

Ioannou GN. The Role of Cholesterol in the Pathogenesis of NASH. Trends Endocrinol Metab. 2016; 27:84–95. [PubMed: 26703097]

Ishimoto T, Lanaspa MA, Rivard CJ, Roncal-Jimenez CA, Orlicky DJ, Cicerchi C, McMahan RH, Abdelmalek MF, Rosen HR, Jackman MR, et al. High-fat and high-sucrose (western) diet induces steatohepatitis that is dependent on fructokinase. Hepatology. 2013; 58:1632–1643. [PubMed: 23813872]

Jolley CD, Dietschy JM, Turley SD. Genetic differences in cholesterol absorption in 129/Sv and C57BL/6 mice: effect on cholesterol responsiveness. Am J Physiol. 1999; 276:G1117–1124. [PubMed: 10330001]

Joshi-Barve S, Barve SS, Amancherla K, Gobejishvili L, Hill D, Cave M, Hote P, McClain CJ. Palmitic acid induces production of proinflammatory cytokine interleukin-8 from hepatocytes. Hepatology. 2007; 46:823–830. [PubMed: 17680645]

Kleiner DE, Brunt EM, Van Natta M, Behling C, Contos MJ, Cummings OW, Ferrell LD, Liu YC, Torbenson MS, Unalp-Arida A, et al. Design and validation of a histological scoring system for nonalcoholic fatty liver disease. Hepatology. 2005; 41:1313–1321. [PubMed: 15915461]

Kohli R, Kirby M, Xanthakos SA, Softic S, Feldstein AE, Saxena V, Tang PH, Miles L, Miles MV, Balistreri WF, et al. High-fructose, medium chain trans fat diet induces liver fibrosis and elevates

plasma coenzyme Q9 in a novel murine model of obesity and nonalcoholic steatohepatitis. Hepatology. 2010; 52:934–944. [PubMed: 20607689]

Liang W, Menke AL, Driessen A, Koek GH, Lindeman JH, Stoop R, Havekes LM, Kleemann R, van den Hoek AM. Establishment of a General NAFLD Scoring System for Rodent Models and Comparison to Human Liver Pathology. PloS one. 2014; 9:e115922. [PubMed: 25535951]

Lisowski L, Dane AP, Chu K, Zhang Y, Cunningham SC, Wilson EM, Nygaard S, Grompe M, Alexander IE, Kay MA. Selection and evaluation of clinically relevant AAV variants in a xenograft liver model. Nature. 2014; 506:382–386. [PubMed: 24390344]

Liu CY, Lv X, Li T, Xu Y, Zhou X, Zhao S, Xiong Y, Lei QY, Guan KL. PP1 cooperates with ASPP2 to dephosphorylate and activate TAZ. J Biol Chem. 2011; 286:5558–5566. [PubMed: 21189257]

Liu F, Lagares D, Choi KM, Stopfer L, Marinkovic A, Vrbanac V, Probst CK, Hiemer SE, Sisson TH, Horowitz JC, et al. Mechanosignaling through YAP and TAZ drives fibroblast activation and fibrosis. Am J Physiol Lung Cell Mol Physiol. 2015; 308:L344–357. [PubMed: 25502501]

Luedde T, Kaplowitz N, Schwabe RF. Cell death and cell death responses in liver disease: mechanisms and clinical relevance. Gastroenterology. 2014; 147:765–783. e764. [PubMed: 25046161]

Machado MV, Michelotti GA, Pereira TA, Xie G, Premont R, Cortez-Pinto H, Diehl AM. Accumulation of duct cells with activated YAP parallels fibrosis progression in non-alcoholic fatty liver disease. J Hepatol. 2015

Mederacke I, Dapito DH, Affo S, Uchinami H, Schwabe RF. High-yield and high-purity isolation of hepatic stellate cells from normal and fibrotic mouse livers. Nat Protoc. 2015; 10:305–315. [PubMed: 25612230]

Mederacke I, Hsu CC, Troeger JS, Huebener P, Mu X, Dapito DH, Pradere JP, Schwabe RF. Fate tracing reveals hepatic stellate cells as dominant contributors to liver fibrosis independent of its aetiology. Nat Commun. 2013; 4:2823. [PubMed: 24264436]

Mitani A, Nagase T, Fukuchi K, Aburatani H, Makita R, Kurihara H. Transcriptional coactivator with PDZ-binding motif is essential for normal alveolarization in mice. Am J Respir Crit Care Med. 2009; 180:326–338. [PubMed: 19498055]

Miura K, Yang L, van Rooijen N, Brenner DA, Ohnishi H, Seki E. Toll-like receptor 2 and palmitic acid cooperatively contribute to the development of nonalcoholic steatohepatitis through inflammasome activation in mice. Hepatology. 2013; 57:577–589. [PubMed: 22987396]

Mu X, Espanol-Suner R, Mederacke I, Affo S, Manco R, Sempoux C, Lemaigre FP, Adili A, Yuan D, Weber A, et al. Hepatocellular carcinoma originates from hepatocytes and not from the progenitor/biliary compartment. J Clin Invest. 2015; 125:3891–3903. [PubMed: 26348897]

Nishio M, Sugimachi K, Goto H, Wang J, Morikawa T, Miyachi Y, Takano Y, Hikasa H, Itoh T, Suzuki SO, et al. Dysregulated YAP1/TAZ and TGF-beta signaling mediate hepatocarcinogenesis in Mob1a/1b-deficient mice. Proc Natl Acad Sci U S A. 2016; 113:E71–80. [PubMed: 26699479]

Ozcan L, Wong CC, Li G, Xu T, Pajvani U, Park SK, Wronska A, Chen BX, Marks AR, Fukamizu A, et al. Calcium signaling through CaMKII regulates hepatic glucose production in fasting and obesity. Cell Metab. 2012; 15:739–751. [PubMed: 22503562]

Piersma B, Bank RA, Boersema M. Signaling in Fibrosis: TGF-beta, WNT, and YAP/TAZ Converge. Front Med (Lausanne). 2015; 2:59. [PubMed: 26389119]

Puche JE, Saiman Y, Friedman SL. Hepatic stellate cells and liver fibrosis. Compr Physiol. 2013; 3:1473–1492. [PubMed: 24265236]

Rawson RB. An ARC light on lipid metabolism. Cell Metab. 2006; 4:181–183. [PubMed: 16950135]

Razzaque MS, Soegiarto DW, Chang D, Long F, Lanske B. Conditional deletion of Indian hedgehog from collagen type 2alpha1-expressing cells results in abnormal endochondral bone formation. J Pathol. 2005; 207:453–461. [PubMed: 16278811]

Rinella ME. Nonalcoholic fatty liver disease: a systematic review. JAMA. 2015; 313:2263–2273. [PubMed: 26057287]

Saito A, Nagase T. Hippo and TGF-beta interplay in the lung field. Am J Physiol Lung Cell Mol Physiol. 2015; 309:L756–767. [PubMed: 26320155]

Seki E, De Minicis S, Gwak GY, Kluwe J, Inokuchi S, Bursill CA, Llovet JM, Brenner DA, Schwabe RF. CCR1 and CCR5 promote hepatic fibrosis in mice. J Clin Invest. 2009; 119:1858–1870. [PubMed: 19603542]

Shimamura T, Fujisawa T, Husain SR, Kioi M, Nakajima A, Puri RK. Novel role of IL-13 in fibrosis induced by nonalcoholic steatohepatitis and its amelioration by IL-13R-directed cytotoxin in a rat model. J Immunol. 2008; 181:4656–4665. [PubMed: 18802068]

Singh S, Allen AM, Wang Z, Prokop LJ, Murad MH, Loomba R. Fibrosis progression in nonalcoholic fatty liver vs nonalcoholic steatohepatitis: a systematic review and meta-analysis of paired-biopsy studies. Clin Gastroenterol Hepatol. 2015; 13:643–654. e641–649. quiz e639-640. [PubMed: 24768810]

Subramanian S, Goodspeed L, Wang S, Kim J, Zeng L, Ioannou GN, Haigh WG, Yeh MM, Kowdley KV, O'Brien KD, et al. Dietary cholesterol exacerbates hepatic steatosis and inflammation in obese LDL receptor-deficient mice. J Lipid Res. 2011; 52:1626–1635. [PubMed: 21690266]

Syn WK, Choi SS, Liaskou E, Karaca GF, Agboola KM, Oo YH, Mi Z, Pereira TA, Zdanowicz M, Malladi P, et al. Osteopontin is induced by hedgehog pathway activation and promotes fibrosis progression in nonalcoholic steatohepatitis. Hepatology. 2011; 53:106–115. [PubMed: 20967826]

Syn WK, Oo YH, Pereira TA, Karaca GF, Jung Y, Omenetti A, Witek RP, Choi SS, Guy CD, Fearing CM, et al. Accumulation of natural killer T cells in progressive nonalcoholic fatty liver disease. Hepatology. 2010; 51:1998–2007. [PubMed: 20512988]

Teratani T, Tomita K, Suzuki T, Oshikawa T, Yokoyama H, Shimamura K, Tominaga S, Hiroi S, Irie R, Okada Y, et al. A high-cholesterol diet exacerbates liver fibrosis in mice via accumulation of free cholesterol in hepatic stellate cells. Gastroenterology. 2012; 142:152–164. e110. [PubMed: 21995947]

Van Rooyen DM, Larter CZ, Haigh WG, Yeh MM, Ioannou G, Kuver R, Lee SP, Teoh NC, Farrell GC. Hepatic free cholesterol accumulates in obese, diabetic mice and causes nonalcoholic steatohepatitis. Gastroenterology. 2011; 141:1393–1403. 1403, e1391–1395. [PubMed: 21703998]

White DL, Kanwal F, El-Serag HB. Association between nonalcoholic fatty liver disease and risk for hepatocellular cancer, based on systematic review. Clin Gastroenterol Hepatol. 2012; 10:1342–1359. e1342. [PubMed: 23041539]

Wouters K, van Gorp PJ, Bieghs V, Gijbels MJ, Duimel H, Lutjohann D, Kerksiek A, van Kruchten R, Maeda N, Staels B, et al. Dietary cholesterol, rather than liver steatosis, leads to hepatic inflammation in hyperlipidemic mouse models of nonalcoholic steatohepatitis. Hepatology. 2008; 48:474–486. [PubMed: 18666236]

Xin M, Kim Y, Sutherland LB, Murakami M, Qi X, McAnally J, Porrello ER, Mahmoud AI, Tan W, Shelton JM, et al. Hippo pathway effector Yap promotes cardiac regeneration. Proc Natl Acad Sci U S A. 2013; 110:13839–13844. [PubMed: 23918388]

Yamada K, Mizukoshi E, Sunagozaka H, Arai K, Yamashita T, Takeshita Y, Misu H, Takamura T, Kitamura S, Zen Y, et al. Characteristics of hepatic fatty acid compositions in patients with nonalcoholic steatohepatitis. Liver Int. 2015; 35:582–590. [PubMed: 25219574]

Younossi ZM, Page S, Rafiq N, Birerdinc A, Stepanova M, Hossain N, Afendy A, Younoszai Z, Goodman Z, Baranova A. A biomarker panel for non-alcoholic steatohepatitis (NASH) and NASH-related fibrosis. Obes Surg. 2011; 21:431–439. [PubMed: 20532833]

Yu FX, Zhao B, Guan KL. Hippo Pathway in Organ Size Control, Tissue Homeostasis, and Cancer. Cell. 2015; 163:811–828. [PubMed: 26544935]

Zanconato F, Cordenonsi M, Piccolo S. YAP/TAZ at the Roots of Cancer. Cancer Cell. 2016; 29:783–803. [PubMed: 27300434]

Zanconato F, Forcato M, Battilana G, Azzolin L, Quaranta E, Bodega B, Rosato A, Bicciato S, Cordenonsi M, Piccolo S. Genome-wide association between YAP/TAZ/TEAD and AP-1 at enhancers drives oncogenic growth. Nat Cell Biol. 2015; 17:1218–1227. [PubMed: 26258633]

Zhao B, Li L, Lei Q, Guan KL. The Hippo-YAP pathway in organ size control and tumorigenesis: an updated version. Genes Dev. 2010; 24:862–874. [PubMed: 20439427]

Zhao B, Ye X, Yu J, Li L, Li W, Li S, Yu J, Lin JD, Wang CY, Chinnaiyan AM, et al. TEAD mediates YAP-dependent gene induction and growth control. Genes Dev. 2008; 22:1962–1971. [PubMed: 18579750]

Highlights

- TAZ/WWTR1 is increased in hepatocytes in human and mouse NASH liver
- Hepatocyte TAZ silencing in steatosis blocks inflammation, cell death, and fibrosis
- Hepatocyte TAZ silencing in NASH reverses inflammation, cell death, and fibrosis
- Hepatocyte TAZ promotes fibrosis by inducing Ihh, a hepatic stellate cell activator

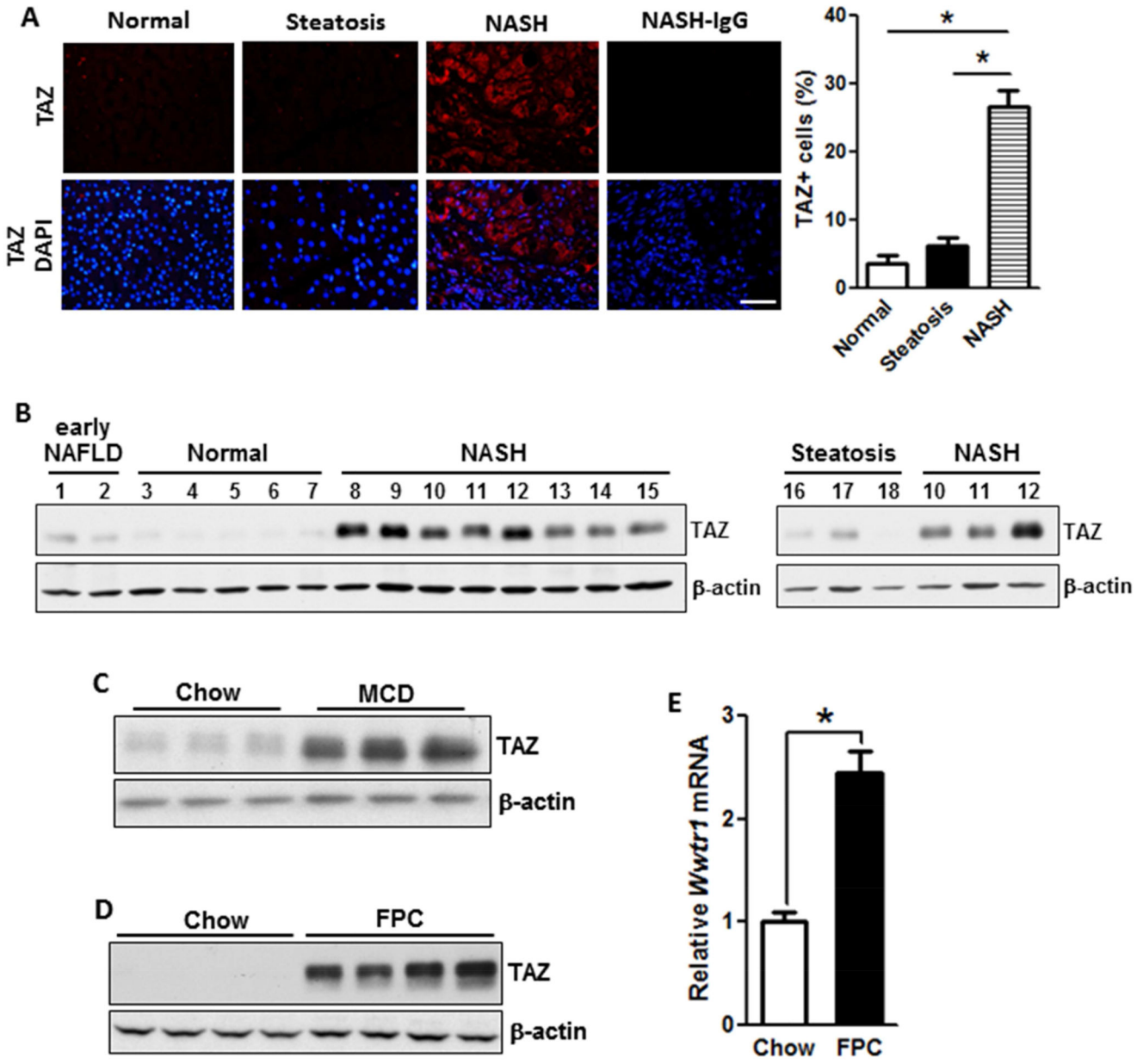

Figure 1. TAZ Levels are Increased in the Livers of Humans and Mice with NASH

(A) TAZ immunofluorescence (red) in normal, steatotic, and NASH human liver sections; DAPI counterstain for nuclei is shown in bottom panels. NASH-IgG refers to control for primary antibody. Bar, 100 μm. The data were quantified as percent TAZ^+ cells relative to total liver cells (*$p < 0.0001$; mean ± SEM; n=7 specimens/group).

(B) Immunoblots of TAZ in early NAFLD, normal, NASH, and steatotic human liver. For sake of comparison, samples #10-12 of NASH from the left blot were re-run with the steatosis samples in the right blot. β-actin was used as loading control.

(C) Immunoblot of liver TAZ in mice fed chow or MCD diet, with β-actin as loading control.

(D) Immunoblot of liver TAZ in mice fed chow or FPC diet, with β-actin as loading control.

(E) Quantification of *Wwtr1* (Taz) mRNA in livers from mice fed chow or FPC diet (*p < 0.0001; mean ± SEM; n=6 mice/group)

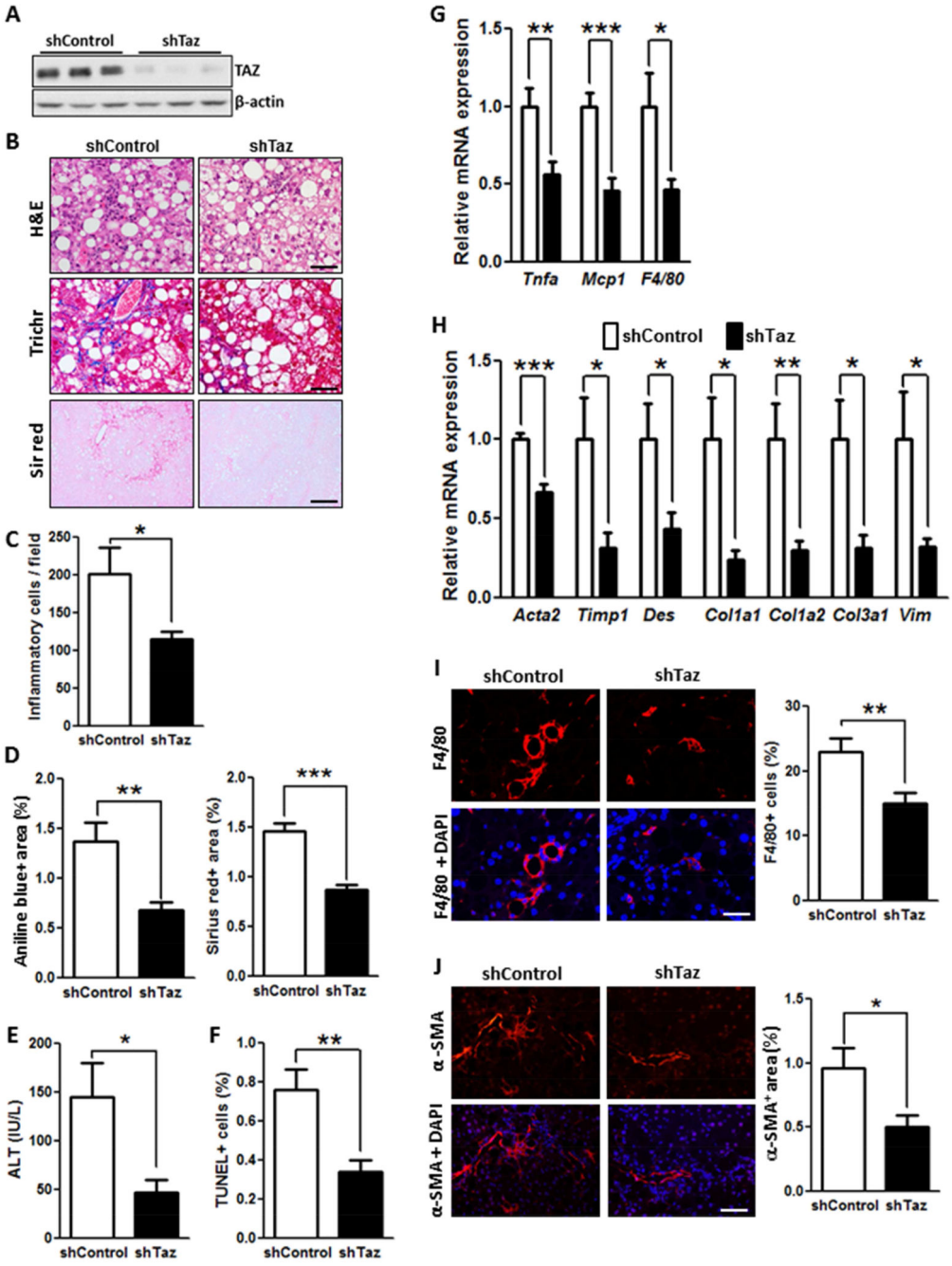

Figure 2. TAZ Silencing Reduces Liver Inflammation, Fibrosis, and Cell Death in FPC-Fed Mice

The following parameters were measured in male C57BL/6J mice treated with AAV8-H1-shTaz or control vector and then fed the FPC diet for 16 weeks (*p < 0.05, **p < 0.01, ***p < 0.0002, mean ± SEM; n=10 mice/group):

(A) Immunoblot of TAZ in liver, with β-actin as loading control.

(B) Staining of liver sections for H&E (upper panels; Bar, 100 μm), Masson's trichrome (Trichr) (middle panels; Bar, 100 μm), and Sirius red (Sir red) (lower panels; Bar, 500 μm).

(C) Hepatic inflammatory cells.

(D) Aniline blue- and Sirius red-positive area.
(E) Plasma ALT.
(F) TUNEL$^+$ cells.
(G) mRNA levels of *Tnfa*, *Mcp1*, and *F4/80* (*Adgre1*).
(H) mRNA levels of the indicated genes related to fibrosis.
(I) F4/80 immunofluorescence (red) and quantification; DAPI counterstain for nuclei is shown in bottom panels; Bar, 100 μm.
(J) α-SMA immunofluorescence (red) and quantification; DAPI counterstain for nuclei is shown in bottom panels; Bar, 100 μm.

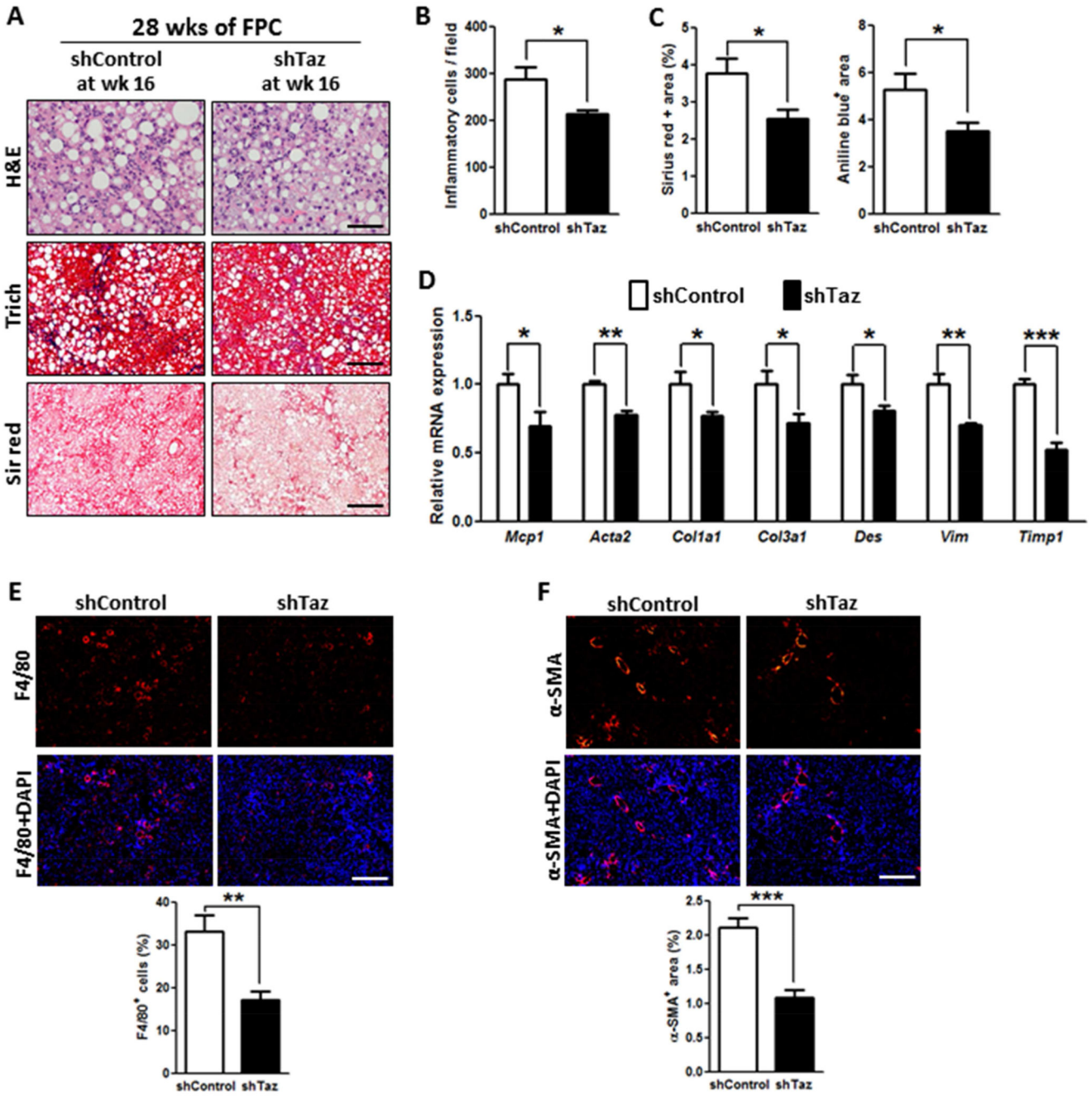

Figure 3. TAZ Silencing After the Development of NASH Reduces Liver Inflammation and Fibrosis in FPC-Fed Mice

The following parameters were measured in male C57BL/6J mice fed the FPC diet for 28 weeks, with AAV8-H1-shTaz or control vector administered at the 16-week time point (*p < 0.05; **p < 0.01, ***p < 0.0001, mean ± SEM; n=5 mice/group):

(A) Staining of liver sections for H&E (upper panels; Bar, 100 μm), Masson's trichrome (Trichr) (middle panels; Bar, 500 μm), and Sirius red (Sir red) (lower panels; Bar, 500 μm).

(B) Hepatic inflammatory cells.

(C) Aniline blue- and Sirius red-positive area.

(D) mRNA levels of *Mcp1*, *Acta2* (α-SMA), *Col1a1*, *Col3a1, Des, Vim and Timp1*.
(E) F4/80 immunofluorescence (red) and quantification; DAPI counterstain for nuclei is shown in bottom panels; Bar, 500 μm.
(F) α-SMA immunofluorescence (red) and quantification; DAPI counterstain for nuclei is shown in bottom panels; Bar, 500 μm.

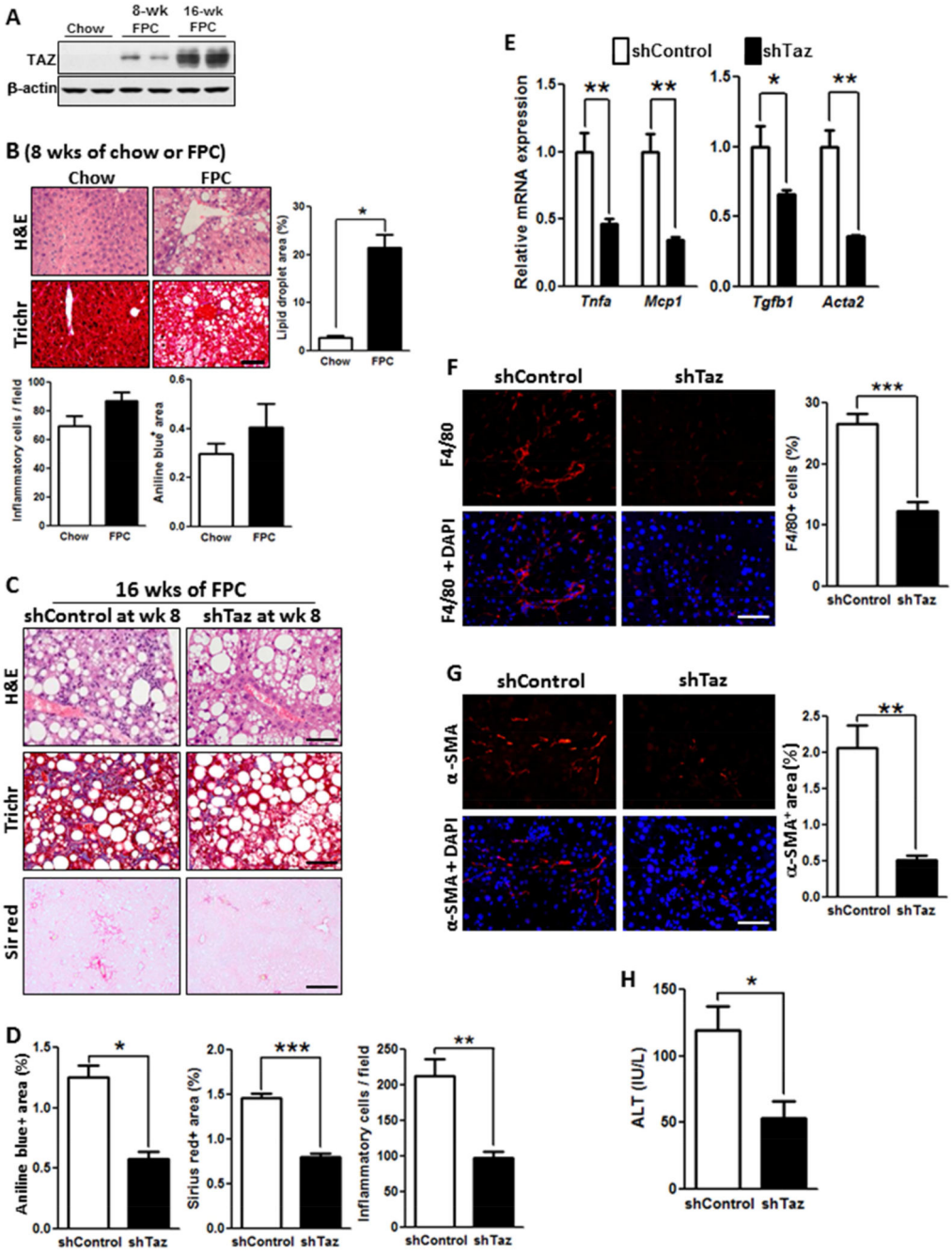

Figure 4. TAZ Silencing After the Development of Steatosis Reduces Liver Inflammation and Fibrosis in FPC-Fed Mice

(A) TAZ immunoblot of liver extracts from C57BL/6J mice fed chow or FPC diet for 8 or 16 weeks.

(B) H&E- and Masson's trichrome (Trich)-stained liver sections and quantified lipid droplet area, inflammatory cells, and aniline blue-positive area for C57BL/6J mice fed chow or FPC diet for 8 weeks. Bar, 100 μm.

(C-H) The following parameters were measured in male C57BL/6J mice fed the FPC diet for 16 weeks, with AAV8-H1-shTaz or control vector administered at the 8-week time point (*p < 0.05; **p < 0.01, ***p < 0.0001, mean ± SEM; n=5 mice/group):
(C) Staining of liver sections for H&E (upper panels; Bar, 100 μm), Masson's trichrome (Trichr) (middle panels; Bar, 100 μm), and Sirius red (Sir red) (lower panels; Bar, 500 μm).
(D) Aniline blue- and Sirius red-positive area and hepatic inflammatory cells.
(E) mRNA levels of *Tnfa*, *Mcp1*, *Tgfb1*, and *Acta2* (α-SMA).
(F) F4/80 immunofluorescence (red) and quantification; DAPI counterstain for nuclei is shown in bottom panels; Bar, 100 μm.
(G) α-SMA immunofluorescence (red) and quantification; DAPI counterstain for nuclei is shown in bottom panels; Bar, 100 μm.
(H) Plasma ALT.

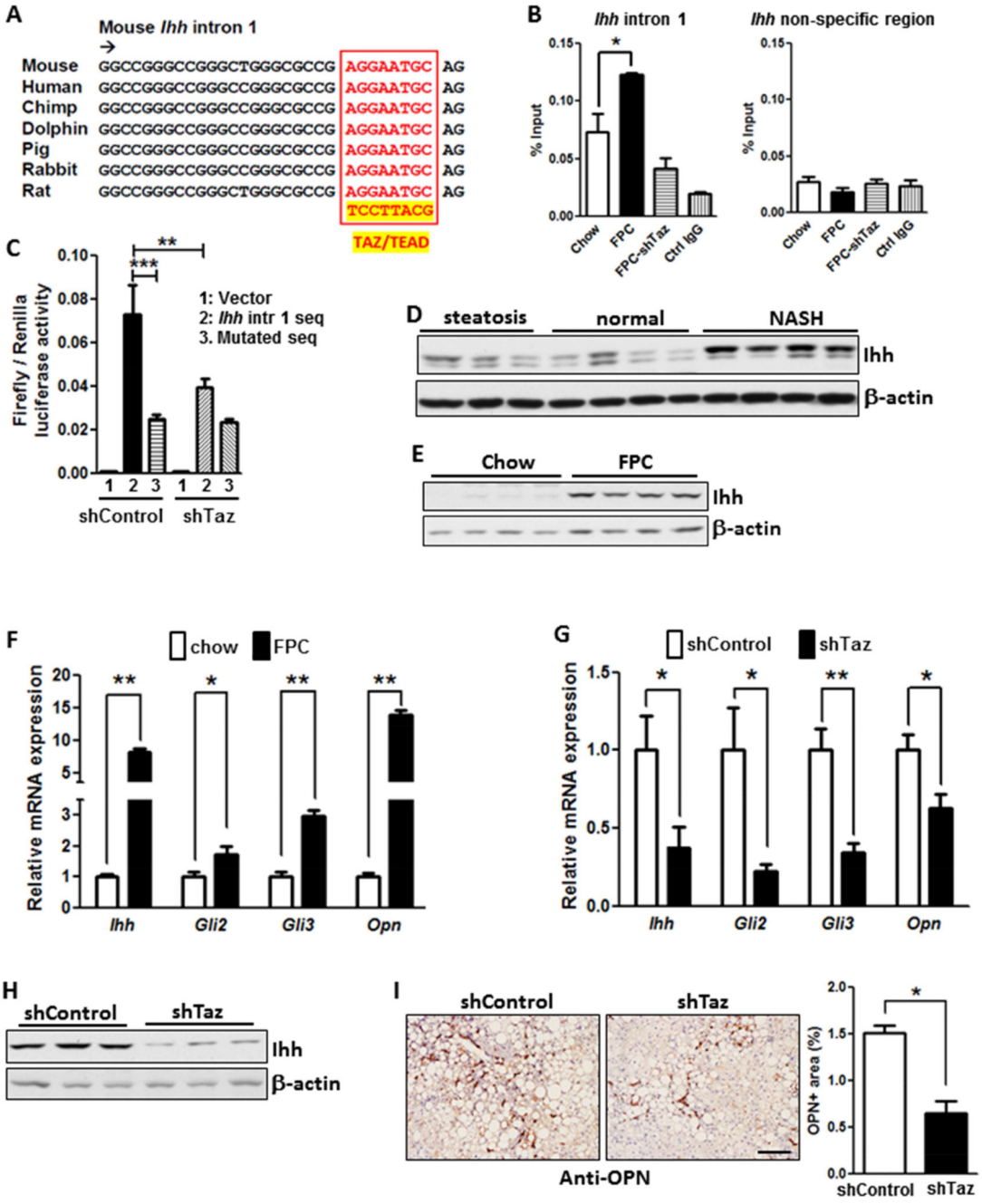

Figure 5. TAZ Induces *Ihh*, and TAZ Silencing Lowers the Expression of Pro-Fibrotic Hedgehog Pathway Genes in the Livers of FPC-Fed Mice

(A) Conserved TAZ/TEAD consensus sequence in intron 1 of the mouse *Ihh* gene.

(B) Liver nuclear extracts from mice fed chow diet or FPC diet for 16 weeks with or without TAZ silencing were subjected to TAZ ChIP analysis using anti-TAZ or IgG control. The intronic region containing the TAZ/TEAD binding sequence, or a non-consensus sequence as control, was amplified by qPCR and normalized to the values obtained from input DNA (*p = 0.03; mean ± SEM; n=3).

(C) A dual-luciferase reporter assay in control and TAZ-silenced AML12 cells was conducted using the *Ihh* intron 1 region in (B), or a mutated version, together with 500 bp of flanking upstream and downstream sequence. (**p < 0.01, ***p < 0.0001; mean ± SEM; n=6).

(D) Immunoblot of Ihh in normal humam livers or those with steatosis or NASH.

(E) Immunoblot of Ihh in the livers of mice fed chow or FPC diet for 16 weeks.

(F) Relative expression of *Ihh*, *Gli2*, *Gli3*, and *Opn* mRNAs in the livers of mice fed chow or FPC diet for 16 weeks (*p < 0.04, **p < 0.0001; mean ± SEM; n=6).

(G) Relative expression of *Ihh*, *Gli2*, *Gli3*, and *Opn* mRNAs in the livers of mice fed the FPC diet for 16 weeks with or without TAZ silencing (*p < 0.05, **p < 0.002; mean ± SEM; n=10).

(H) Immunoblot of Ihh in the livers of mice fed the FPC diet for 16 weeks with or without TAZ silencing.

(I) OPN immunohistochemistry and quantification in the livers of mice fed the FPC diet for 16 weeks with or without TAZ silencing (*p < 0.0001; mean ± SEM; n=10); Bar, 200 μm.

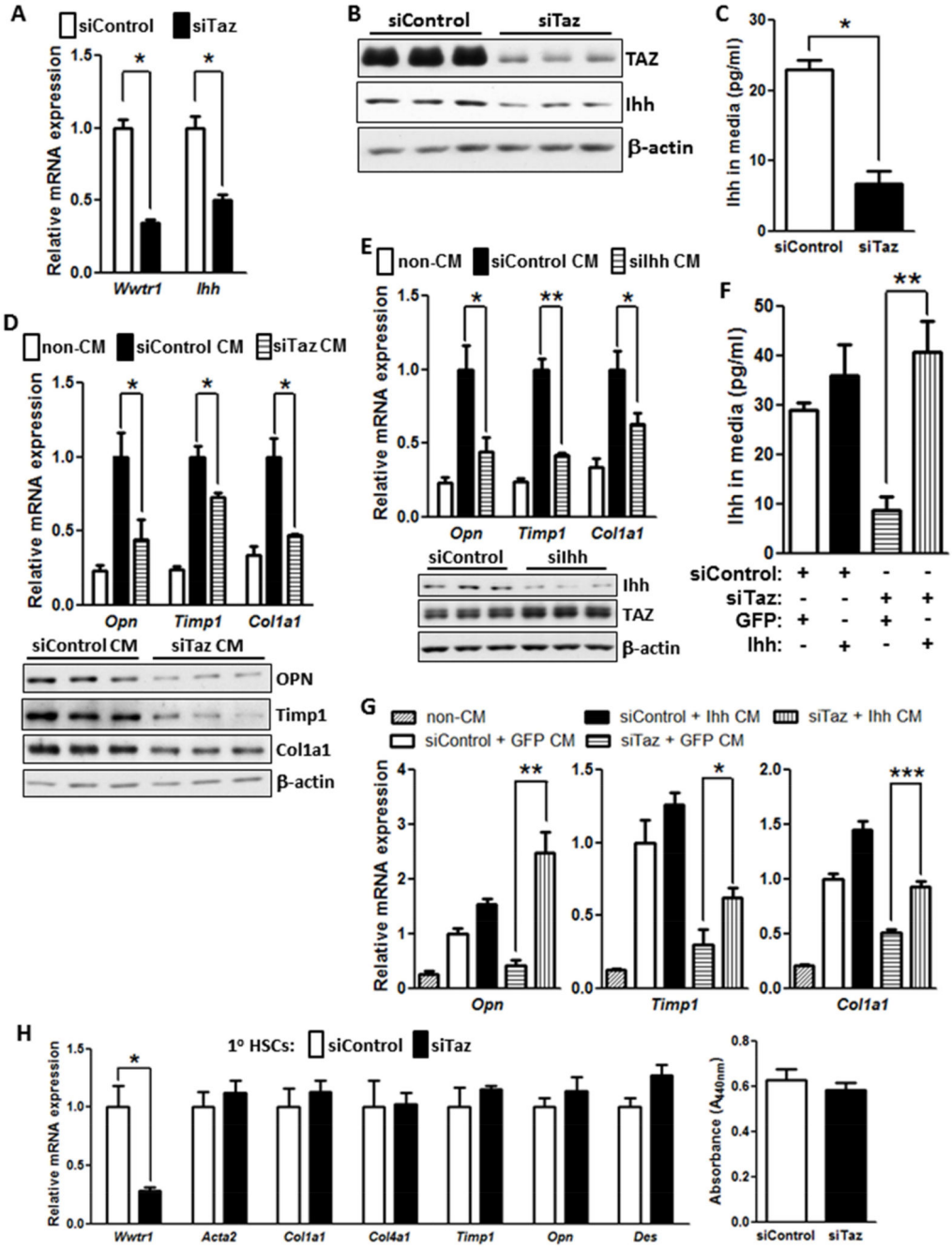

Figure 6. TAZ-Induced Hepatocyte Ihh Increases the Expression of Fibrosis-Related Genes in Hepatic Stellate Cells

(A) Expression of *Wwtr1* and *Ihh* mRNA in control and TAZ-silenced AML12 cells (*p < 0.0003; mean ± SEM; n=3).

(B) Immunoblot of TAZ and Ihh in control and TAZ-silenced AML12 cells.

(C) Ihh concentrations, assayed by ELISA, in the media of control and TAZ-silenced AML12 cells (*p < 0.003; mean ± SEM; n=3).

(D) Primary hepatic stellate cells (HSCs) were incubated for 72 h with conditioned medium (CM) obtained from control or Taz-silenced AML12 cells or with medium not exposed to

cells (non-CM). The HSCs were then assayed for *Opn*, *Timp1*, and *Col1a1* mRNA (upper panel; *p < 0.05; mean ± SEM; n=4) and the respective proteins by immunoblot (lower panel).

(E) HSCs were incubated for 72 h with non-CM or CM obtained from control or Ihh-silenced AML12 cells and then assayed for *Opn*, *Timp1*, and *Col1a1* mRNA (*p < 0.04; **p < 0.0001, mean ± SEM; n=4). Immunoblot of Ihh and TAZ in siIhh-treated and control AML12 cells is shown below the graph.

(F) Control or Taz-silenced AML12 cells that were transduced with a plasmid encoding Ihh or control GFP. Aliquots of the four sets of conditioned medium were assayed for Ihh by ELISA (*p < 0.002; mean ± SEM; n=3).

(G) HSCs were incubated with conditioned media from the 4 sets of cells in (F) or with non-CM and then assayed for *Opn*, *Timp1*, and *Col1a1* mRNA (*p < 0.05; **p < 0.004, ***p < 0.0004, mean ± SEM; n=4). Note that bars 2 and 3 for *Opn* and *Col1a1* are significantly different at p < 0.05.

(H) Primary HSCs were activated by culturing for 72 h in medium containing 10% FBS and then treated with siControl or siTaz duplex, followed by culturing in the same medium for an additional 48 h. The cells were then assayed for *Wwtr1*, *Acta2*, *Col1a1*, *Col4a1*, *Timp1*, *Opn*, and *Des* mRNAs or cell proliferation. For the proliferation assay, the cells were synchronized by overnight culture in medium containing 0.2% FBS and then cultured an additional 48 h in medium containing 10% FBS. The cells were incubated with WST-1, and absorbance at 440 nm was measured to assess cell number.

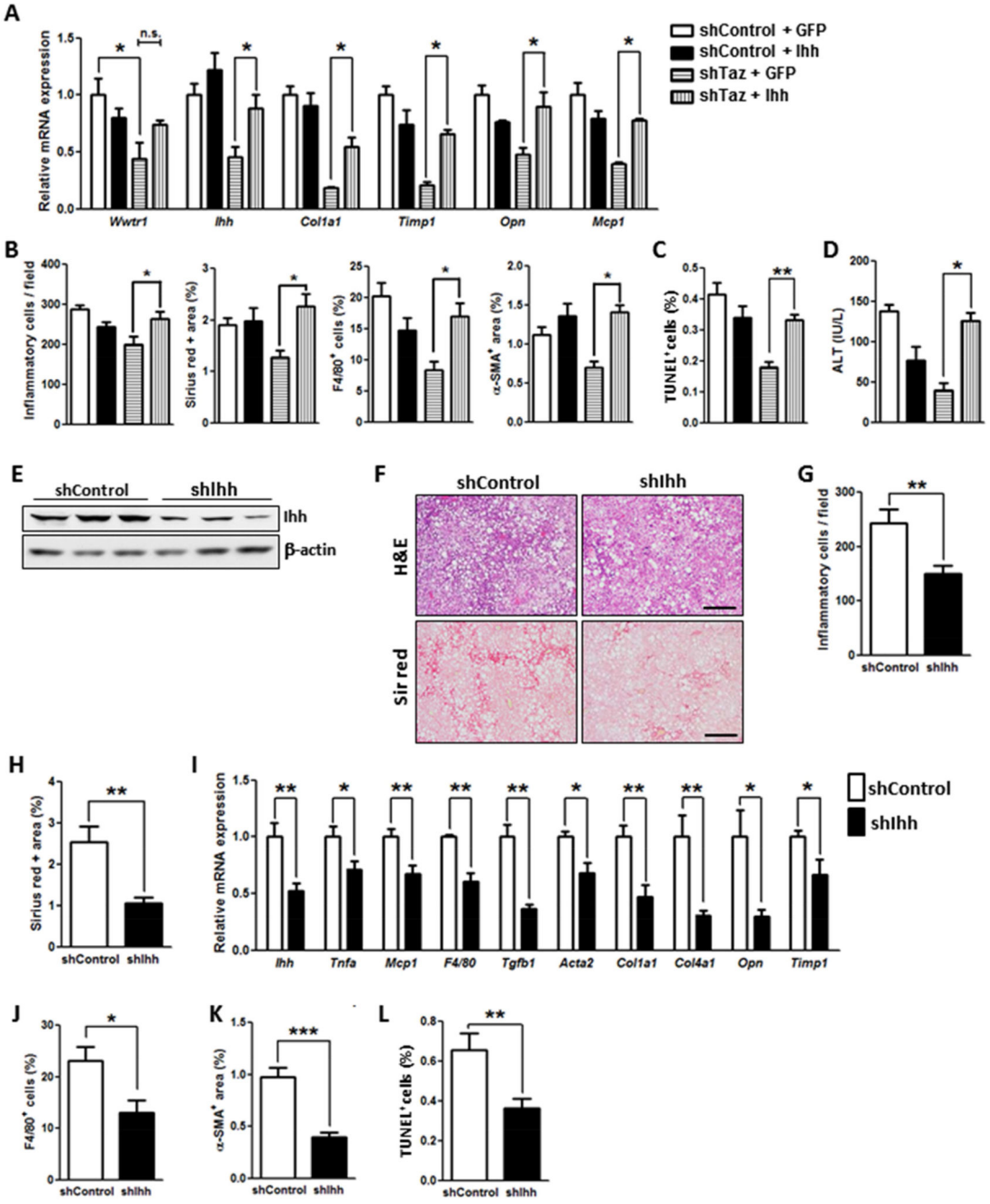

Figure 7. Ihh Restoration in Taz-Silenced FPC-Fed Mice Promotes NASH Features, and Ihh Silencing Reduces NASH Features

(A-D) The following parameters were measured in male C57BL/6J mice treated with AAV8-H1-shTaz or control vector and then overexpressed Ihh or GFP by AAV8 vector, fed the FPC diet for 16 weeks (*$p < 0.05$, **$p < 0.01$, mean ± SEM; n=6 mice/group):

(A) mRNA levels of *Wwtr1*, *Ihh*, *Col1a1*, *Timp1, Opn*, and *Mcp1.*

(B) Quantification of inflammatory cells, Sirius red positive area, $F4/80^+$ cells, and α-SMA^+ area.

(C) $TUNEL^+$ cells.

(D) Plasma ALT.

(E-L) The following parameters were measured in male C57BL/6J mice treated with AAV8-H1-sh*Ihh* or control vector and then fed the FPC diet for 16 weeks (*p < 0.05, **p < 0.01, ***p < 0.0001, mean ± SEM; n=5 mice/group):

(E) Immunoblot of Ihh, with β-actin as loading control.

(F) Staining of liver sections for H&E (upper panels; Bar, 500 μm) and Sirius red (Sir red) (lower panels; Bar, 500 μm).

(G) Hepatic inflammatory cells.

(H) Sirius red-positive area.

(I) mRNA levels of the indicated genes related to inflammation and fibrosis.

(J) $F4/80^+$ cells.

(K) α-SMA^+ area.

(L) $TUNEL^+$ cells.